Available online at **www.joac.info**

ISSN: 2278-1862

Journal of Applicable Chemistry

2019, 8 (1): 380-388

(International Peer Reviewed Journal)

Investigation of the Structure, Thermal and Magnetic Properties of $Cu_{0.8}Zn_{0.2}Fe_2O_4$ Ferrite Material

Manyazewal Kebede Woldemedhin*

Department of Physics, College of Natural Science, Arba Minch University,
Arba Minch, **ETHIOPIA**
Email: manukebede@gmail.com

Accepted on 16th January, 2019

ABSTRACT

Spinel cubic $Cu_{0.8}Zn_{0.2}Fe_2O_4$ magnetic material was synthesized by two steps solid state reaction method. The thermogravimetric analysis-differential thermal analysis (TGA/DTA), x-ray powder diffraction (XRD) and vibrational sample magnetometer (VSM) characterization techniques were utilized to investigate the thermal, structural and magnetic properties of $Cu_{0.8}Zn_{0.2}Fe_2O_4$ sample. Analysis of TGA-DTA confirmed that 900℃ is the appropriate temperature for synthesizing $Cu_{0.8}Zn_{0.2}Fe_2O_4$ sample using CuO, ZnO and Fe_2O_3 as precursors. From the structural analysis by XRD, it was found that the synthesized sample exhibited single phase with cubic spinel structure having space group of Fd-3m. The lattice parameter and crystal size of $Cu_{0.8}Zn_{0.2}Fe_2O_4$ sample were found to be 8.428Å and 38.54 nm, respectively. Different structural parameters such as x-ray density, bulk density, porosity, particle size, hopping lengths in both tetrahedral and octahedral sites, etc. were estimated from XRD data. The magnetic characterization was conducted at room temperature and found that $Cu_{0.8}Zn_{0.2}Fe_2O_4$ sample exhibited a ferromagnetic behavior with a saturation magnetization of 66.7 emu g^{-1}. From the obtained hysteresis loop, the remnant magnetization (Mr) and coercivity (Hc) of $Cu_{0.8}Zn_{0.2}Fe_2O_4$ sample were estimated and are found to 16.5 emu g^{-1} and 45 Gauss, respectively, indicating that $Cu_{0.8}Zn_{0.2}Fe_2O_4$ is a soft magnetic material.

Graphical Abstract

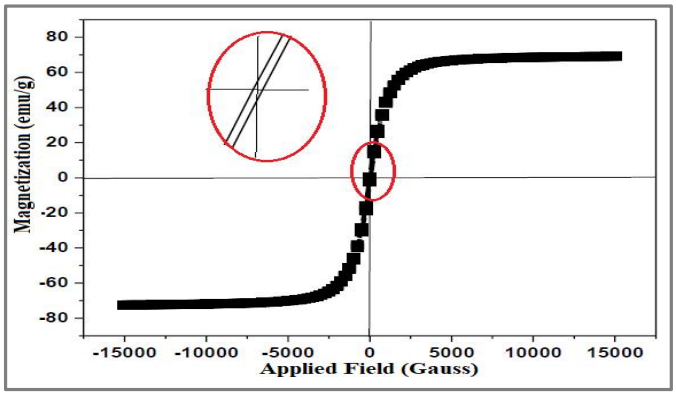

The room temperature magnetic hysteresis loop of $Cu_{0.8}Zn_{0.2}Fe_2O_4$ ferrite.

Keywords: Characterization, Solid state reaction method, Thermal property, Magnetic property.

INTRODUCTION

Spinel ferrites are a class of magnet ceramic materials with the formula AB_2O_4, where A and B represent different metal cations, including iron cations [**1, 2**]. These materials have a significant role in advancing industrial and scientific applications with major benefits in various sectors with a large variety of applications in electronic and telecommunication industries [**3, 4**]. Spinel ferrites research and innovation attracts scientific community, mainly due to their versatile physical, mechanical, chemical and structural properties and due to their technological applications in magnetic sensors, biosensors, photo - catalysts, nanoelectronics, biomedical [**5, 6**]. Like most other ceramics, spinel ferrites are hard and brittle behaviors [**7**]. These materials have attracted the attention of chemists, physicists as well as technologists, since they exhibit excellent magnetic and electrical properties. It means that the magnetic, electric and dielectric properties possessed by ferrites made them more attractive to the current field of science and technology. These properties of ferrites depend on several factors, including cation distribution in the two tetrahedral and octahedral cites, method of preparation, heating conditions, chemical composition, crystallite size, etc [**8, 9**].

The magnetic behavior of ferrites is quite different from ferromagnetism, which is exhibited by metallic materials. Ferrite exhibits ferrimagnetism behavior due to the super-exchange interaction between electrons of cations and oxygen ions [**10, 11**]. The opposite spins in ferrite results in the lowering of magnetization compared to ferromagnetic metals where the spins are parallel. Due to the intrinsic atomic level interaction between cations and oxygen ions, ferrites have higher resistivity compared to ferromagnetic metals [**12**]. This enables the ferrite to find applications at higher frequencies and makes it technologically very valuable. Their magnetic properties can also greatly depend on the type of compositions in ferrite compounds.

Copper ferrite ($CuFe_2O_4$) is an interesting material and has been widely used for various applications, such as catalysts for environment, gas sensor, and hydrogen production [**13, 14**]. This type of ferrite belongs to the inverse spinel structure with 8 Cu^{2+} ions occupying octahedral B-site while 16 Fe^{3+} ions ideally occupy equally the tetrahedral (A-sites) and octahedral (B-sites) sites of the unit cell [**14, 15**]. Many varieties of synthesis methods have been used in the production of spinel ferrites. Among several synthesis methods, solid state reaction, sol-gel, auto-combustion, precipitation and hydrothermal methods are commonly employed techniques to produce cupper ferrite materials [**16-18**]. In the last decade, solid state reaction method has become an increasingly useful technique for synthesizing all kinds of materials. Solid state reaction method has some advantages over other methods such as the effect of processing simplicity, low cost, mass production, etc.

In this study, solid state reaction method was employed for the synthesis of $Cu_{0.8}Zn_{0.2}Fe_2O_4$ spinel ferrite. Different characterization techniques such as TGA/DTA, XRD and VSM were employed to study the structural, thermal and magnetic properties of this material.

MATERIALS AND METHODS

Synthesis Procedures: $Cu_{0.8}Zn_{0.2}Fe_2O_4$ magnetic material was synthesized by solid state reaction method using precursors CuO, ZnO and Fe_2O_3. Initially, a mixture of stoichiometric MgO, CuO and Fe_2O_3 were ground in agate mortar for about 2h before adding methanol. After thorough homogenizing with some methanol added, the mixed powder was also ground again in agate mortar for 1h. Further, the obtained powder material was heated at 550°C for two hours in air with a heating and cooling rate of 5°C min^{-1}. The heated powder was ground again for one hour and calcined at 900°C for 12 h in air with a heating and cooling rate of 5°C min^{-1}. Finally, this calcined powder material was ground for an hour to obtain $Cu_{0.8}Zn_{0.2}Fe_2O_4$ fine powder. Detail of the synthesis procedure is shown in the following flow chart.

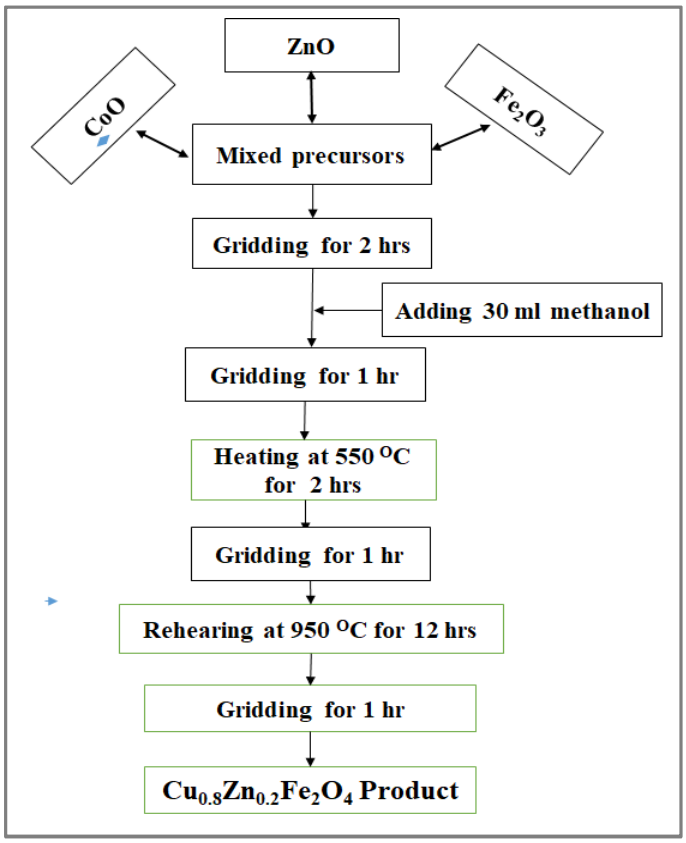

Figure 1. Flow diagram of sample preparation by solid state reaction.

Material Characterizations: The TGA/DTA analysis of $Cu_{0.8}Zn_{0.2}Fe_2O_4$ material was conducted using DTG-60H thermal analysis instrument. For this characterization, about 17 mg sample was used and the sample was heated from room temperature to 1000°C in the TGA furnace at a heating and cooling rate of 10°C per min in nitrogen atmosphere. The structure of $Cu_{0.8}Zn_{0.2}Fe_2O_4$ material in the form of powder was identified by XRD using a Phillips XPERT-PRO diffractometer fitted with Cu Kα radiation (λ = 1.54060 Å) between diffraction angles 2θ = 20° and 80°. The magnetic property study of the synthesized sample was conducted using vibrating sample magnetometer system (VSM 3900 Princeton) instrument. The external magnetic field was applied in the range of -50,000 to 50,000 Gauss.

RESULTS AND DISCUSSION

Thermal analysis: Thermo-gravimetric analysis (TGA) along with the differential thermal analysis (DTA) of the prepared sample was carried out to identify the annealing temperature necessary for the ferrite formation. Figure 2 shows the TGA and DTA curves for the mixture of CuO, ZnO and Fe_2O_3 raw materials to form $Cu_{0.8}Zn_{0.2}Fe_2O_4$ compound heated up to a temperature of 1000°C in oxygen atmosphere. As seen from the figure, different exothermic peaks are observed from the DTA curve, indicating the exothermic nature of the reaction of CuO, ZnO and Fe_2O_3 raw materials to form $Cu_{0.8}Zn_{0.2}Fe_2O_4$ compound.

On the other hand, TGA curve shows three weight loss regions. Initially, a minor weight loss of 2.3% in the temperature range from room temperature to 173°C is identified. This may be attributed to the removal of methanol used during grinding and moisture absorbed by the dry powder during storage. This effect is identified by endodermic peaks at 62 and 126°C. Further, a significant weight loss of about 9.8% is obtained from 173°C to 380°C, which is attributed to the reaction of CuO, ZnO

and Fe_2O_3 raw materials to form $Cu_{0.8}Zn_{0.2}Fe_2O_4$ compound. This effect is also identified by a sharp endodermic peak at 318°C. Minor weight loss of 1.2% is detected from 497°C to 815°C, which may be probably the reaction of the remaining undecomposed part of the raw materials. After a temperature of 684°C, the TGA curve becomes more flattened, indicating stable phase formation of $Cu_{0.8}Zn_{0.2}Fe_2O_4$ compound. The total weight loss up to 900°C is found be 10.6%. This study reveals that the crystalline formation of $Cu_{0.8}Zn_{0.2}Fe_2O_4$ is completed before 900°C. From this TGA and DTA study, it can be deduced that 900°C is the appropriate temperature for synthesizing pure phase $Cu_{0.8}Zn_{0.2}Fe_2O_4$ compound by solid state reaction method using CuO, ZnO and Fe_2O_3 raw materials. Similar results were observed by different authors [19].

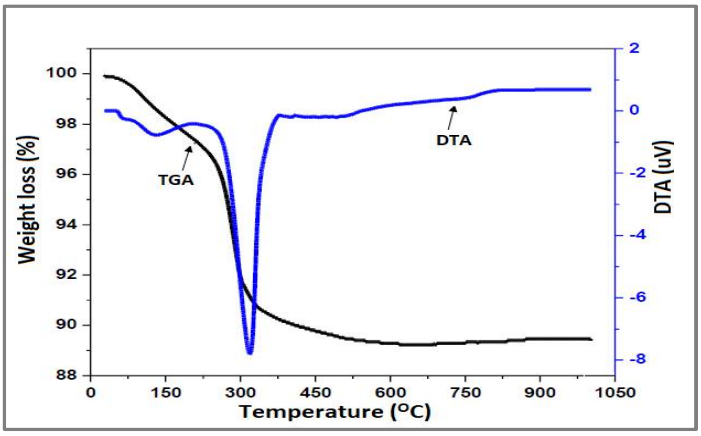

Figure 2. TGA/DTA analysis of $Cu_{0.8}Zn_{0.2}Fe_2O_4$.

XRD study: The X-ray powder diffraction (XRD) pattern of $Cu_{0.8}Zn_{0.2}Fe_2O_4$ ferrite material synthesized by solid state reaction method at a temperature of 900°C for 12 h in air is shown in figure 3. As it can be seen in the figure, sharp, intense, broadening and well-defined peaks are found, indicating high crystallinity nature of the compound. The broadening of the peaks is attributed to the formation of smaller particle size of the sample. The XRD peaks observed at **2θ values of 29.4, 34.9, 36.4, 42.4, 48.6, 52.9, 56.5, 62.2, 65.4, 70.7, 73.7 and 74.7°** are corresponding to the planes (220), (311), (222), (400), (422), (311), (422), (511), (440), (531), (620), (533) and (622), respectively which provides a clear evidence for the formation of cubic spinel phase with Fd-3m space group. Further, the obtained XRD peaks are in coherence well with the Joint Committee on Powder Diffraction Standards (JCPDS) Card no. 35-782. These diffraction peaks also provide clear evidence of the formation of single ferrite phase in $Cu_{0.8}Zn_{0.2}Fe_2O_4$ sample.

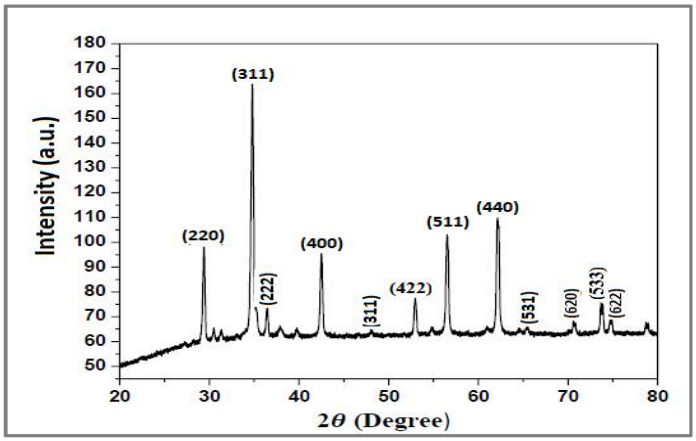

Figure 3. XRD analysis of $Cu_{0.8}Zn_{0.2}Fe_2O_4$.

In this study, the lattice constant (a) and unit cell volume (V) of $Cu_{0.8}Zn_{0.2}Fe_2O_4$ sample were calculated from (400) XRD peak using the equations;

$$a = d\sqrt{h^2 + k^2 + l^2} \quad \text{--(1)}$$

$$V = a^3 \quad \text{--(2)}$$

Where d is the inter-planar spacing and hkl are Miller indices. The crystal size (D) of $Cu_{0.8}Zn_{0.2}Fe_2O_4$ sample was calculated from (111) XRD peak using Debye-Scherer formula [**2, 7**];

$$D = \frac{0.9\lambda}{\beta \cos\theta} \quad \text{--(3)}$$

Where λ is the wavelength of X-ray, β is the full width at half maximum (FWHM) of the diffraction (111) peak and θ is the Braggs' angle. The obtained results are summarized in table 1. It is identified that the lattice parameter and the unite cell volume of $Cu_{0.8}Zn_{0.2}Fe_2O_4$ sample are found to be 8.428Å and 598.65Å^3, respectively. Moreover, the calculated crystal size of this sample is also found to be 38.54 nm, which reveals the nanostructure of the synthesized compound. Prabhu *et al.* [**20**] have found that the lattice parameter of $CuFe_2O_4$ compound is 8.4nm, which is slightly smaller than the value of $Cu_{0.8}Zn_{0.2}Fe_2O_4$ sample (8.428Å). This effect is associated with the larger ionic radius of Zn^{2+} (0.74Å) than Cu^{2+}(0.72Å) [**21**], leading to the larger in lattice parameter, unit cell volume and crystal size of $Cu_{0.8}Zn_{0.2}Fe_2O_4$ sample.

Table 1. 2θ value, d-spacing, lattice constant, cell volume, FWHM and crystal size of the synthesized sample

Sample	2θ value for (400) (degree)	d-spacing for (400) (Å)	Lattice Constant a (Å)	Unite Cell Volume V (Å)^3	FWHM (radian)	Crystal Size from (311) (nm)
$Cu_{0.8}Zn_{0.2}Fe_2O_4$	42.36	2.107	8.428	598.65	0.0386	38.54

The bulk density ρ_B of $Cu_{0.8}Zn_{0.2}Fe_2O_4$ sample was determined by measuring the volume and mass of the sintered ferrite sample using the relation

$$\rho_b = \frac{m}{A\,D} \quad \text{--(4)}$$

Where m is the mass of the pellet, A and D are the cross sectional area and thickness of the pellet, respectively.

The X-ray density of the synthesized sample was calculated using the relation;

$$\rho_{ex} = \frac{nM}{N_A a^3} \quad \text{--(5)}$$

Where n is the number of formula units per unit cell of spinel lattice, M is the molecular weight of the sample, N_A is the Avogadro number (6.022×10^{23} mol^{-1}) and a is the lattice constant. The surface area (S) and porosity (P) of both samples were calculated using the relations;

$$S = \frac{6}{D\,\rho_{ex}} \quad \text{--(6)}$$

$$P = \frac{\rho_{ex} - \rho_B}{\rho_{ex}} \quad \text{--(7)}$$

The constant 6 is called the form factor for spherical particles. The obtained results are summarized at table 2. As seen from the table, the calculated values of the x-density, bulk density, specific surface area and porosity of $Cu_{0.8}Zn_{0.2}Fe_2O_4$ sample are found to be 4.4 g cm^{3-1}, 5.3 g cm^{3-1}, 29.4 m^2 $g^{-1}$and 17%, respectively. It is observed that the obtained value of the X-ray density of $Cu_{0.8}Zn_{0.2}Fe_2O_4$ sample is greater than its corresponding bulk density, which is commonly observed in porous materials. This reveals the existence and formation of pores in the samples during the synthesis and calcination processes. A similar result has been obtained by Maria et al. in Cu-Zn ferrite [22].

The hopping lengths (L_A and L_B) in both tetrahedral and octahedral sites of $Cu_{0.8}Zn_{0.2}Fe_2O_4$ sample were calculated using the relation;

$$L_A = \frac{a\sqrt{3}}{4} \quad \text{--(8)}$$

$$L_B = \frac{a\sqrt{2}}{4} \quad \text{--(9)}$$

Where 'a' is the lattice parameter and 'u' is oxygen positional parameter. The theoretical bond length of tetrahedral A-site (d_{AL}) and octahedral B-site (d_{BL}) of $Cu_{0.8}Zn_{0.2}Fe_2O_4$ sample were also calculated using the relations;

$$d_{AL} = a\sqrt{3}(u - 0.25) \quad \text{--(10)}$$

$$d_{BL} = a\sqrt{3u^2 - \frac{11}{4}u + \frac{43}{64}} \quad \text{--(11)}$$

Table 2. Summary of different structural parameter values of the synthesis compound

Sample	Bulk density ρ_b (gm cm^{3-1})	X-ray density ρ_{ex} (gm cm^{3-1})	Surface area S (m^2 gm^{-1})	Porosity P (%)	L_A (nm)	L_B (nm)	d_{AL} (nm)	d_{BL} (nm)
$Cu_{0.8}Zn_{0.2}Fe_2O_4$	4.4	5.3	29.4	17	0.365	0.298	0.19	0.21

The calculated values of L_A, L_B,d_{AL} and d_{BL} are summarized in table 2. The hopping lengths in the tetrahedral and octahedral sites of $Cu_{0.8}Zn_{0.2}Fe_2O_4$ are found to be 0.365 and 0.298 nm, respectively. This indicates that the hopping length in tetrahedral site is larger than that of the octahedral site, which is in good agreement with previous study [23]. The bond length of tetrahedral A-site and octahedral B-site of $Cu_{0.8}Zn_{0.2}Fe_2O_4$ are 0.19 and 0.21 nm, respectively. This indicates that the bond length of octahedral B-site is larger than the tetrahedral A-site in $Cu_{0.8}Zn_{0.2}Fe_2O_4$.

Magnetic property study: Figure 4 shows the hysteresis curve of $Cu_{0.8}Zn_{0.2}Fe_2O_4$ ferrite material prepared by solid state reaction method at room temperature. As seen from the figure, the magnetic hysteresis loop for ferrite sample attributes to s-shaped narrow hysteresis loops with low coercivity value, suggesting the soft ferrite or superparamagnetic behavior of the material. It can also be observed that the magnetization of $Cu_{0.8}Zn_{0.2}Fe_2O_4$ ferrite increases rapidly with increasing the applied magnetic field up to 2,500 Gauss. Beyond this applied field, the magnetization increases slowly and becomes saturated. This indicates that $Cu_{0.8}Zn_{0.2}Fe_2O_4$ sample is in ferromagnetic state at room temperature.

From the obtained hysteresis loop, the magnetic parameters like saturation magnetization (Ms), remnant magnetization (Mr) and coercivity (Hc) of $Cu_{0.8}Zn_{0.2}Fe_2O_4$ sample were estimated and the obtained results are indicated in table 3. It is found that $Cu_{0.8}Zn_{0.2}Fe_2O_4$ ferrite sample shows Ms, Mr

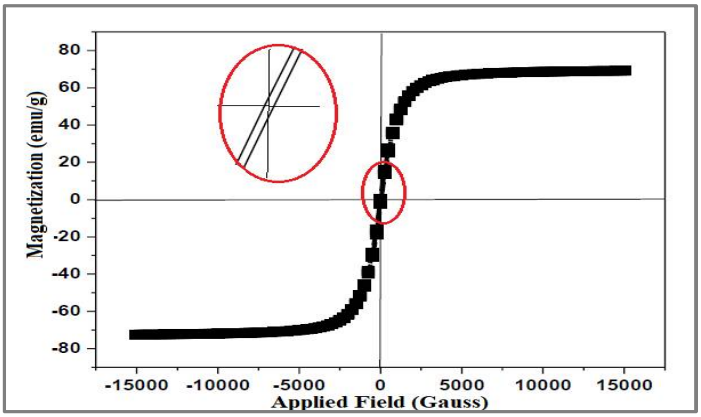

Figure 4. The room temperature magnetic hysteresis loop of $Cu_{0.8}Zn_{0.2}Fe_2O_4$ferrite.

and Hc values of 66.7 emu g^{-1}, 16.5 emu g^{-1} and 45 Gauss, respectively. This indicates that the synthesized material processes low values of H_c and H_r, showing that $Cu_{0.8}Zn_{0.2}Fe_2O_4$ is soft magnetic material. From the obtained values of H_r and H_c, the loop squareness ratio (Mr/Ms) was also calculated and it is found to be 0.5.

Table 3. Saturation magnetization, coercivity and retentivity of the synthesized ferrite sample.

Material	Saturation Magnetization Ms (emu g^{-1})	Retentivity Mr (emu g^{-1})	Coercivity Hc (Gauss)
$Cu_{0.8}Zn_{0.2}Fe_2O_4$	66.7	16.5	45

APPLICATION

From the obtained values of H_r and H_c, the loop squareness ratio (Mr/Ms) was also calculated and it was found to be less than 0.5. Thus, it can be suggested that the synthesized $Cu_{0.8}Zn_{0.2}Fe_2O_4$ ferrite can be used for several technological applications such as cores, soft magnets and coils with low inductance.

CONCLUSION

$Cu_{0.8}Zn_{0.2}Fe_2O_4$ ferrite sample were successfully synthesized by two steps solid-state reaction method. From TGA/DTA study, it was suggested that 900°C is the appropriate temperature for synthesizing pure phase $Cu_{0.8}Zn_{0.2}Fe_2O_4$ compound by solid state reaction method using CuO, ZnO and Fe_2O_3 raw materials. XRD analysis revealed that the synthesized samples adopted cubic spinel structure and it belong to Fd-3m space group. Using Debye-Scherer formula, the crystal size of the synthesized sample was found to be 38.54 nm, which indicated the nanoparticle nature of $Cu_{0.8}Zn_{0.2}Fe_2O_4$ compound. From the magnetic property study, it was found that $Cu_{0.8}Zn_{0.2}Fe_2O_4$ ferrite sample delivered 66.7 emu g^{-1}, 16.5 emu g^{-1} and 45 Gauss values of Ms, Mr and Hc, respectively. This revealed that the synthesized material has soft magnetic nature.

ACKNOWLEDGEMENTS

The authors are gratefully acknowledged to Dr. Paulos Taddesse and Department of Chemistry for assisting and providing some facilities to conduct this research work.

REFERENCES

[1]. M. Gunay, H. Erdemi, A. Baykal, H. Sozeri, M. S. Toprak, Triethylene glycol stabilized $MnFe_2O_4$ nanoparticle: Synthesis, magnetic and electrical characterization, *Mater Res Bull.*, **2013**, 48, 1057-1064.

[2]. M. Srivastava, S. Chaubey, A. K. Ojha, Investigation on size dependent structural and magnetic behavior of nickel ferrite nanoparticles prepared by sol–gel and hydrothermal methods, *Mater Chem and Phys.*, **2009**, 118, 174-180.

[3]. S. Daliya, Mathew, R. S. Juang, An overview of the structure and magnetism of spinel ferrite nanoparticles and their synthesis in micro emulsions, *Chem Eng J.*, **2007**, 129, 51-65.

[4]. J. Mayekar, V. Dhar, S. Radha, Synthesis, characterization and magnetic study of Zinc Ferrite Nanoparticles, *Int J Innov Res Sci and Eng.*, **2016**, 5, 137-161.

[5]. M. A. Gabal, Y. M. Al Angari, Effect of diamagnetic substitution on the structural, magnetic and electrical properties of $NiFe_2O_4$, *Mater Chem and Phys.*, **2009**, 115, 578–584.

[6]. D. Varshney, K. Verma, Substitutional effect on structural and dielectric properties of $Ni_{1-x}A_xFe_2O_4$ (A = Mg, Zn) mixed spinel ferrites, *Mater Chem and Phys.*, **2013**, 140, 412-418.

[7]. V. V. Dhole, Structural and micro structural study of Zirconium (Zr^{4+}) doped Nickel Ferrite ($NiFe_2O_4$) Nanoparticles, *Int Adv Res J Sci, Eng and Tech.*, **2016,** 3, 76-78.

[8]. M. Hashim, Alimuddin, S. Kumar, S. E. Shirsath, R. K. Kotnala, Synthesis and characterizations of Ni^{2+} substituted Cobalt Ferrite Nanoparticles, *J. Shah, R. Kumar, Mater Chem and Phys.*, **2013**, 139, 364-374.

[9]. S. M. Patange, S. E Shirsath, S. P, Jadhav, V. S. Hogade, S. R. Kamble, K. M. Jadhav, Elastic properties of Nanocrystalline Aluminum substituted Nickel Ferrites prepared by co-precipitation method, *J Mol Struct.*, **2013**, 1038, 40-44.

[10]. V. J. Angadi, B. Rudraswamy, K. Sadhana, S.R. Murthy, K. Praveena, Effect of Sm^{3+}-Gd^{3+} on structural, electrical and magnetic properties of Mn-Zn ferrites synthesized via combustion route, *J. alloys and comp.*, **2016**, 656, 5-12.

[11]. L. Zhao, H. Zhang, Y. Xing, S. Song S. Yu, W. Shi, X. Guo, J. Yang, Y. Lei, F. Cao, Studies on the magnetism of Cobalt Ferrite Nanocrystals synthesized by hydrothermal method, *J. Solid State Chem,* **2008**, 181, 245-252.

[12]. K. V. Babu, G.Satyanarayana, B. Sailaja, G. V. S. Kumar, K. Jalaiah, M. Ravi, Structural and magnetic properties of $Ni_{0.8}M_{0.2}Fe_2O_4$ (M = Cu, Co) nano-crystalline ferrites, *Results in Phys.*, **2018**, 9, 55-62.

[13]. Y. Dinga, L. Zhua, N. Wanga, H. Tang, Sulfate radicals induced degradation of tetrabromo bisphenol A with nanoscaled magnetic $CuFe_2O_4$ as a heterogeneous catalyst of peroxymonosulfate, *App Cat B: Env.*, **2013**, 129, 153-162.

[14]. K. Verma, A. Kumar, D. Varshney, Effect of Zn and Mg doping on structural, dielectric and magnetic properties of tetragonal $CuFe_2O_4$,*Current Applied Phys.*, **2013**, 13, 467-473.

[15]. D. H. Kumar Reddy, Y.-S. Yun, Spinel ferrite magnetic adsorbents: Alternative future materials for water purification, *Coord Chem Rev.,* **2016**, 315, 90-111.

[16]. E .R. Kumar, R. Jayaprakash, J. Chandrasekaran, Effect of fuel ratio and the impact of annealing temperature on particle size, magnetic and dielectric properties of manganese substituted $CuFe_2O_4$ nanoparticles, *Superlattices and Microstructures*, **2013**, 64, 343–353.

[17]. K. Praveena, B. Radhika, S. Srinath, Dielectric and magnetic properties of $NiFe_{2-x}Bi_xO_4$ nanoparticles at microwave frequencies prepared via co-precipitation method, *Procedia Eng.*, **2014**, 76, 1-7.

[18]. T. Sodaee, A. Ghasemi, R. S. Razavi, Cation distribution and microwave absorptive behavior of gadolinium substituted cobalt ferrite ceramics, *J All and Comp.*, **2017**, 706, 133-146.

[19]. P. P. Hankare, V. T. Vader, N. M. Patil, S. D. Jadhav, U. B. Sankpal, M. R. Kadam, B. K. Chougule, N. S. Gajbhiye, Synthesis, characterization and studies on magnetic and electrical properties of Mg ferrite with Cr substitution, *Mater Chem and Phys.*, **2009**, 113, 233-238.

[20]. D. Prabhu, A. Narayanasamy, K. Shinoda, B. Jeyadeven, J.M. Greneche, K. Chattopadhyay, Grain size effect on the phase transformation temperature of nanostructured $CuFe_2O_4$, *J Appl Phys*., **2011**, 109, 013532 1-7.
[21]. S. Alamolhoda, S. M. Mirkazemi, N. Benvidi, T. Shahjooyi, The effects of Cu and Zn dopants on phase constituents, magnetic properties and microstructure of Nickel Ferrite, *J Nanosci Nanotechnol*., **2016**, 12, 131-137.
[22]. K. H. Maria, S. Choudhury, M. A. Hakim, Structural phase transformation and hysteresis behavior of Cu-Zn ferrites, *Inter Nano Lett.*, **2013**, 42, 1-10.
[23]. N. Najmoddin, A. Beitollahi, H. Kavas, S. M. Mohseni, H. Rezaie, J. Åkerman, M. S. Toprak, XRD cation distribution and magnetic properties of mesoporous Zn-substituted $CuFe_2O_4$,*Ceram Int.*, **2014**, 40, 3619-3625.